Journal of Nanotechnology and Innovative Materials

Research Article

Nanoengineered Material Architecture for Improved Durability and Sealing of Bidirectional Two-Way Ball Valves in Waxy Particle-Laden Oil Pipelines

Tatyana Huseynova

Department of Industrial Engineering, Azerbaijan State Oil and Industry University, Baku, Azerbaijan

Received: 05.08.2026 Accepted: 26.09.2026 Published: 12.10.2026
https://doi.org/10.54414/PQOZ1595

Copyright: © 2026 by the authors. Licensee: Journal of Nanotechnology and Innovative Materials, Western Caspian University, Baku, Azerbaijan. This article is an open-access article distributed under the terms and conditions of the Creative Commons Attribution 4.0 International License (CC BY 4.0).

Abstract

Two-way ball valves used in oil and gas pipelines are exposed to a coupled damage system rather than to a single wear mechanism. Local jets during throttling promote cavitation and particle erosion; repeated opening and closing produce adhesive and abrasive wear at the ball seat interface; elastic and viscoelastic deformation alters bidirectional contact pressure; and wax accumulation can increase actuation torque or prevent complete seating. This paper develops a functionally zoned nanoengineered material architecture for a trunnion-mounted two-port ball valve that must isolate pressure from either direction. The architecture does not assume that one nanomaterial can protect every component. Instead, each damage zone is assigned a candidate system and a separate verification route. A dense polished micro nano structured WC–10Co–4Cr coating is proposed as the lead option for the ball sealing band and metallic scraper ring. Duplex nitriding with diamond-like carbon and CrN or CrCN thin films are retained as comparators where a thin low-friction surface is preferable. Graphene nanoplatelet PEEK and hBN PEEK are proposed for controlled screening as primary seat materials, while graphene-modified FKM is considered for the secondary elastomeric seal. A graphene oxide phytic acid film is included only as an exploratory antiwax treatment for protected noncontact flow surfaces. Two noninterchangeable validation envelopes are defined: a field screening line with an 89 mm bore, 0.6 to 1.2 MPa pressure, 50 to 60 °C temperature, 250 m³ per day flow, 2 to 5 percent wax and 132 mg per litre solids; and a DN500 PN100 structural qualification valve with a differential pressure up to 10 MPa. The proposed methodology couples transient CFD, nonlinear contact FEA, coating and polymer coupon tests, wax deposition experiments, and bidirectional valve cycling. Published coupon and valve data motivate the candidate materials, but no unmeasured valve-level performance is claimed. The principal contribution is a falsifiable selection framework that connects hydraulic damage maps and seat contact pressure to material zoning and qualification decisions.

Keywords: ball valve, nanocomposite WC–CoCr, PEEK fluoroelastomer, cavitation erosion, wax deposition, bidirectional sealing

Highlights

- A damage-driven five-zone nanoengineered architecture is proposed for a bidirectional two-way ball valve
- Micro nano WC–10Co–4Cr is selected as the lead hard coating for the ball sealing band and scraper ring
- Graphene PEEK and graphene FKM are treated as screening candidates that require creep aging and leakage qualification
- An antiwax graphene oxide film is restricted to protected noncontact surfaces and is not placed on the sealing band
- Field screening and DN500 PN100 structural qualification conditions are maintained as separate evidence envelopes

1 Introduction

A two-way ball valve is a two-port shutoff device in which a bored spherical obturator rotates between open and closed positions. In the present study, the term bidirectional describes the isolation requirement: the

closed valve must retain pressure when either pipeline side is pressurized. This distinction is important because hydraulic symmetry does not guarantee mechanical symmetry. Seat springs, pressure-energized cavities, support ring stiffness, machining tolerances, and friction can create different contact pressure fields for the two pressure directions. Pipeline valve design and qualification are governed at system level by API Specification 6D and its ISO supplement ISO 14313, while the present material study adds a damage-focused layer to those requirements [1], [2].

The dissertation problem addressed here is the improvement of two-way ball valve construction for oil and gas pipelines. Earlier stages of the work identified two coupled design objectives. The first is hydraulic: the port and cavity geometry should suppress unnecessary separation, recirculation, local velocity amplification, cavitation susceptibility, and transient pressure loading. The second is tribological and structural: the seat support system should maintain an adequate but not excessive contact pressure, limit concentrated stress, and preserve sealing after repeated cycling. Large ball valve simulations show that closure angle strongly reorganizes the jet and wake, while finite element investigations of bidirectional seats identify the support ring and geometric discontinuities as critical stress zones [3], [4], [5]. Consequently, geometry, preload, and surface engineering must be optimized together.

Conventional material selection often treats the valve as a uniform corrosion and wear problem. That approach is inadequate for a waxy particle-laden service. The ball sealing band experiences high Hertzian-type contact, sliding, and third-body abrasion. The scraper ring encounters deposits and entrained solids. The PEEK primary seat is sensitive to temperature-dependent modulus, creep, transfer film formation, and damage at its leading edge. The FKM secondary seal must resist swelling, gas decompression, and compression set. Protected bore surfaces may accumulate wax but carry little sealing contact. These zones require different combinations of hardness, toughness, low friction, chemical stability, compliance, and surface energy.

Nanoengineered materials can change these combinations through a refined carbide distribution, nanoscale multilayers, solid lubricant platelets, or tortuous diffusion paths. Their use is nevertheless not automatically beneficial. A hard coating with inadequate toughness can crack; a thin film can detach from an insufficiently supported substrate; graphene agglomeration can create leak paths or reduce polymer elongation; and an antiwax film can be removed by particles. A recent high-pressure ball valve failure investigation is especially instructive: coating spallation generated hard debris that intensified third body abrasion, whereas a redesigned seat combined with nitriding and a diamond-like carbon surface endured substantially more cycles in that specific test programme [6]. This evidence supports an interface system approach rather than a catalogue-based choice of fashionable materials.

The objective of this paper is therefore to formulate a research-ready nanoengineered architecture for the dissertation valve, rank the candidate systems, define their permitted locations and establish a validation sequence. The paper is deliberately written as a design and experimental framework. Literature values are used to justify screening decisions, but they are not transferred directly into predicted valve life or leakage. The hypotheses are intended to be tested under the actual contact pressures, fluid composition, temperature, and cycling history of the valve.

2 Valve Architecture and Operating Envelopes

2.1 Reference construction

The reference construction is a trunnion mounted full bore valve with two independently loaded seats. Each side uses a metallic scraper element, a PEEK primary sealing member, and an FKM O-ring as the secondary seal. The trunnion arrangement transfers pressure-induced ball force to the bearings and body instead of relying on seat support alone. For bidirectional isolation, both seat assemblies must tolerate the high-pressure and low-pressure roles. The nanomaterial concept preserves this architecture and changes only selected surfaces or formulations, which makes comparison with the qualified baseline possible.

Figure 1 shows the proposed functional zoning. WC–10Co–4Cr is placed on the metallic sealing and scraping zones because they require a thick load-bearing barrier against abrasion and cavitation. The primary polymer seat and secondary elastomer remain compliant elements and are modified through low-concentration nanofillers rather than through brittle surface layers. The antiwax coating is physically separated from the sealing band. DLC and CrN-based systems are comparators, not additional layers automatically stacked over

WC–CoCr. This prevents an unsupported coating hierarchy and permits adhesion failure to be evaluated independently.

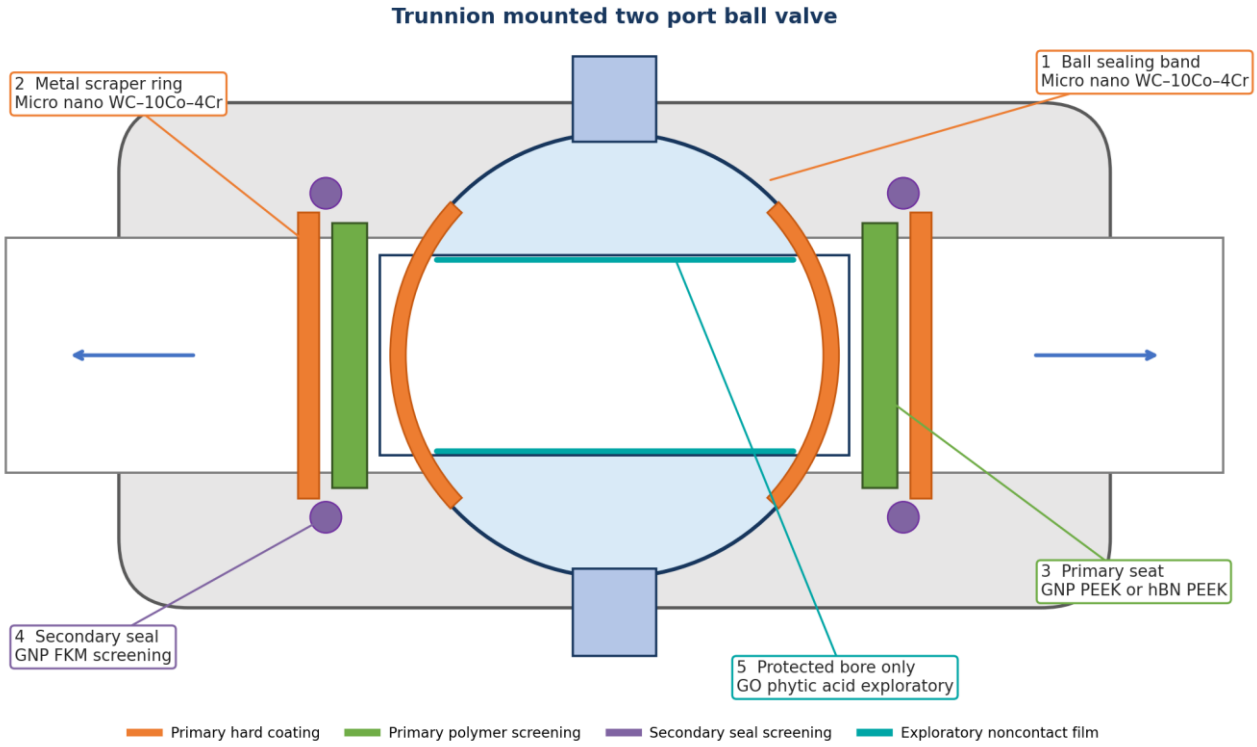


Figure 1 Functionally zoned material architecture for the reference two-way ball valve.

2.2 Separate validation envelopes

Two sets of operating information have been developed during the dissertation and must not be merged into one artificial duty point. Envelope A is a representative produced fluid line used to screen hydraulic behaviour, wax deposition and particle effects. Envelope B is the structural and sealing qualification case for a large valve. The 10 MPa differential pressure of Envelope B must not be assigned to the 89 mm line unless a future project specification explicitly does so. Table 1 preserves this separation.

Table 1 Noninterchangeable operating envelopes used in the proposed research programme.

Parameter	Envelope A	Envelope B
Purpose	Field and flow screening	Structural and sealing qualification
Nominal size	Pipe internal diameter assumed as 89 mm for preliminary calculation	DN500 trunnion-mounted ball valve
Pressure	0.6 to 1.2 MPa line pressure	PN100 class with differential pressure up to 10 MPa
Temperature	50 to 60 °C	To be applied at the specified design and test temperatures
Volumetric flow	250 m³ per day	Qualification flow to be defined by the valve test rig
Fluid density	Approximately 880 kg per m³	Test medium density defined for each hydraulic case
Wax content	2 to 5 percent by the stated field basis	Not automatically transferred to structural pressure tests
Entrained solids	132 mg per litre	Dedicated erosion concentration and size distribution required

Parameter	Envelope A	Envelope B
Seat package	Used to select representative fluids and deposits	Metal scraper, PEEK primary seat, FKM secondary O-ring
Open bore velocity	Approximately 0.465 m per second when 89 mm is the flowing diameter	Not inferred from Envelope A
Open item	Previously supplied oil and water viscosity values require confirmation of units and test temperature	Allowable stresses, leakage class and cycle count require project specification

For Envelope A, converting 250 m³ per day gives a flow rate of approximately 0.00289 m³ per second. Division by the area of an 89 mm circular bore gives an average full open velocity near 0.465 m per second. This average does not exclude damaging local flow. During partial closure, the effective flow area contracts sharply and the jet velocity can become many times greater than the pipe average. Cavitation assessment must therefore use the local pressure and velocity fields rather than a single full bore number.

3 Coupled Failure Mechanisms and Quantitative Indicators

3.1 Hydraulic loss, cavitation, and particle erosion

The pressure loss coefficient provides a geometry-normalized comparison of port shapes and opening angles. With a consistent reference velocity and density, it is defined by Equation 1. A lower value in the fully open position is desirable, but minimizing loss alone is insufficient because a narrow high-speed jet can shift damage to the seat edge or body cavity.

$$K = \frac{\Delta p}{\frac{1}{2}\rho U^2} \quad (1)$$

Cavitation risk is screened using the local cavitation number in Equation 2, where the reference pressure must be stated, and the vapour pressure must correspond to fluid composition and temperature. Multiphase produced fluids require sensitivity analysis because dissolved gas and light hydrocarbons change inception behaviour. A CFD cavitation model should be used to rank designs, followed by an erosion test; it should not be treated as an exact life predictor.

$$\sigma = \frac{p_{\mathrm{ref}} - p_v}{\frac{1}{2}\rho U^2} \quad (2)$$

Particle erosion depends on impact velocity, incidence angle, particle size and shape, concentration, and the target material response. In a closing valve, the highest velocity does not necessarily coincide with the highest erosion because the impact direction and residence time differ around the upstream seat, ball edge, and downstream cavity. A Lagrangian particle model can identify candidate hot spots, but its erosion coefficients must be calibrated with representative solids.

3.2 Contact pressure wear and leakage

A bidirectional seat must maintain a continuous contact band under pressure applied from either side. Li et al. found that high stress developed around the seat support ring and sharp corners in a large fully welded ball valve, and that the effective contact region changed at low pressure [3]. The useful design variable is therefore not only peak contact pressure but its minimum value, circumferential variation, and position relative to the fluid boundary. Equation 3 defines a coefficient of variation for the nodal contact pressure values within the intended sealing band.

$$CV_p = \frac{\mathrm{SD}(p_c)}{\mathrm{mean}(p_c)} \quad (3)$$

The seal design must satisfy both sides of Equation 4. The minimum local pressure must exceed the pressure-assisted sealing requirement with an appropriate project safety factor, while the maximum pressure must remain below the temperature- and medium-dependent allowable contact stress of the seat system. Excess preload can reduce leakage initially but increases torque, polymer creep, and coating damage.

$$p_{c,\min} \geq S_p \Delta p \quad ; \quad p_{c,\max} \leq p_{\mathrm{allow}}(T, \mathrm{medium}) \quad (4)$$

Wear results should be normalized by load and sliding distance only when the wear mechanism and contact geometry make that comparison meaningful. The specific wear rate in Equation 5 is suitable for coupon screening, while valve-level assessment should use loss of sealing geometry, leakage, and torque.

$$k_s = \frac{V_w}{F_N s} \quad (5)$$

3.3 Wax deposition and incomplete seating

Wax affects the valve in three ways. It changes the effective roughness and flow area, increases the force required to scrape the ball, and can become trapped at the seat interface. Laboratory studies demonstrate that surface roughness and alloy type can alter wax deposit thickness and mass, but the direction and magnitude depend on thermal conditions and oil composition [7],[8]. The antiwax problem must therefore be tested under controlled wall temperature, bulk temperature, shear rate, cooling history, and water fraction. A low adhesion flow surface is valuable only if it remains attached and does not contaminate the seal.

Table 2 Damage zones, candidate material systems and principal qualification risks.

Valve zone	Dominant damage	Candidate system	Selection rationale	Main risk to disprove
Ball sealing band	Sliding contact, particles, local cavitation, corrosion	Polished micro nano WC–10Co–4Cr by HVOF or fine feedstock HVAF	Dense load-bearing carbide network and documented valve coating practice [9], [10],[11], [12].	Residual stress, carbide dissolution, pores, edge cracking, finish-induced leakage
Ball sealing band comparator	Low friction sliding and repeated cycling	Nitrided substrate plus DLC as one duplex system	Ball valve cycle evidence and low friction potential [6], [13].	Thin film support adhesion pinholes debris after spallation
Thin film comparator	Adhesive wear and corrosion-assisted cavitation	CrN or CrCN	Hard protective film with measurable cavitation response [14].	Brittle cracking, substrate deformation, coating thickness sensitivity
Metal scraper ring	Deposit cutting, particle abrasion, edge loading	Micro nano WC–10Co–4Cr with a controlled edge radius	Hardness plus fracture toughness and established thermal spray processing [9], [10], [11], [12].	Chipping at sharp edge, excessive counterface wear
Primary PEEK seat	Creep, transfer film, abrasion, thermal expansion	Low-loading GNP PEEK as lead screen; hBN PEEK or WS_2 PEEK as comparators	Graphene and solid lubricant fillers can modify friction, wear, and thermal transport [15], [16], [17].	Agglomeration reduced ductility; leakage paths altered creep and recovery
Secondary FKM O-ring	Swelling, compression set, tear, permeation, gas decompression	Dispersed graphene nanoplatelet FKM	Graphene-filled FKM studies report improved mechanical and barrier related performance [18], [19].	Poor dispersion, hardening, reduced elongation, unverified rapid gas decompression resistance

Valve zone	Dominant damage	Candidate system	Selection rationale	Main risk to disprove
Protected bore and cavity	Wax nucleation and adhesion	GO phytic acid film as exploratory treatment	Strong coupon-level wax inhibition reported in water containing waxy oil [20].	Abrasion durability adhesion water fraction dependence chemical stability
Stem and trunnion journals	Fretting boundary lubrication corrosion	DLC or CrN-based thin film after substrate hardening	Low friction comparator for supported contacts [13], [14].	Edge delamination and dimensional tolerance change

4 Candidate Nanoengineered Material Systems

4.1 Micro nano WC CoCr for metallic sealing zones

WC–CoCr is already used as a wear-resistant valve coating, so the research question is not whether the generic chemistry is hard. It is whether a controlled micro-nano or fine feedstock structure can provide the required combination of density, toughness, surface finish, and residual stress on the actual ball and scraper geometry. Bobzin et al. investigated fine feedstock HVAF coatings for valves with the aim of reducing post-processing. Their work used porosity and as-sprayed roughness as key process outputs and showed that powder route and spray parameters strongly affect electrochemical and mechanical performance [9]. This is directly relevant because grinding a large spherical surface is costly and can expose pores or introduce waviness.

Ding et al. compared micro nano and conventional WC–10Co–4Cr coatings in a sodium chloride cavitation test. The micro-nano coating had low reported porosity, and its steady cavitation erosion rate was about one-half of the conventional coating in that coupon test [10]. Hong et al. likewise studied a near nanostructured HVOF WC–10Co–4Cr coating in saline cavitation [11]. Huang et al. examined slurry erosion of a micro-nano WC–CoCr coating in NaCl medium [12]. Together, these studies justify prioritizing the micro-nano carbide system when cavitation and solids coexist, but they do not establish a valve service life. The coating must be sprayed on the actual substrate and heat-treatment conditions, then finished to a leakage-compatible surface and tested in rolling sliding seat contact.

Two process routes should be compared. HVOF is the reference route with the most direct micro-nano cavitation evidence. HVAF with fine feedstock is a near-net-shape route intended to reduce oxide formation and post-processing. The decision should be based on a multi-response window: porosity, carbide retention, hardness, fracture toughness, bond strength, residual stress, achievable spherical roughness, and leakage after cycling. A very high hardness result should not override visible edge cracking or low adhesion.

4.2 DLC and chromium nitride-based comparators

Diamond-like carbon offers low friction and chemical inertness but is usually much thinner than a thermally sprayed carbide coating. Cheng and Jiang found that DLC improved the cavitation erosion response of stainless steel, while delamination was governed by adhesion and coating defects [13]. For a valve, this means that DLC is most credible on a hard, well-supported substrate and in a contact that does not plastically deform. The 2026 ball valve investigation by Zhang et al. reinforces the point: their improved combination of substrate nitriding, DLC, and a modified seat geometry survived at least 7500 cycles without visible leakage under their stated high-pressure test, whereas the original coating system failed much earlier [6]. The result is promising but inseparable from the geometry and substrate changes.

CrN and CrCN are retained as comparators because they provide a metallic nitride-based alternative with different toughness and thermal stability. Cavitation research on CrN and CrCN indicates that hardness alone is not the best predictor; the H^3 over E^2 index, cracking response, and adhesion must be considered [14]. In this programme, DLC and CrN-based films should first be tested on small spherical or ring specimens manufactured from the actual ball and journal substrate. They should not be deposited over WC–CoCr without a separately engineered interlayer and adhesion study.

4.3 Graphene and solid lubricant modified PEEK

PEEK is attractive for the primary seat because it combines temperature capability, chemical resistance, and sufficient compliance for a polymer-assisted seal. Its weakness is not a single low material property but the interaction of creep, thermal expansion, edge stress, and abrasive wear. Graphene nanoplatelets can

improve stiffness, thermal transport, and tribological behaviour when they are dispersed and bonded effectively. Puértolas et al. studied the mechanical and tribological properties of graphene nanoplatelet PEEK composites and showed that filler loading changes both reinforcement and frictional response [15]. Kalin et al. compared graphene-, WS_2-, and carbon nanotube-filled PEEK, demonstrating that nanofiller type and test conditions determine the wear mechanism [16].

The lead screening family should therefore be neat PEEK and PEEK with 0.5, 1.0, and 2.0 mass percent graphene nanoplatelets. These levels are proposed design of experiment factors, not claimed optima. A separate hBN PEEK family should be studied because hBN can act as a solid lubricant and a thermal conductor without electrical conductivity. A hybrid carbon fibre and hBN literature system has shown low friction and wear in laboratory testing [17], but introducing fibres can make seat machining, anisotropy, and edge integrity more complex. It is preferable to qualify one filler family at a time before considering a hybrid.

Selection must include compression creep and recovery under the contact pressure histories obtained from FEA. A formulation that gives low pin-on-disk wear but develops excessive permanent set can lose the sealing band after pressure removal. Conversely, a stiffer formulation may reduce extrusion but require higher manufacturing precision and spring preload. The decisive test is bidirectional leakage after thermal aging and cycling, supported by profilometry and microscopy of the seat edge and transfer film.

4.4 Graphene-modified FKM for the secondary seal

The FKM O-ring is a secondary barrier and should not be used to compensate for inadequate primary seat contact. Graphene nanoplatelets can create a tortuous permeation path and reinforce an elastomer at modest loading. Liu et al. developed fluoroelastomer graphene nanocomposites for sealing applications, while Wei et al. studied graphene oxide-integrated fluoroelastomer after high-temperature petroleum oil exposure [18], [19]. These studies support screening but do not replace service qualification because filler dispersion, cure system, hardness, and oil composition can change swelling and compression set.

A practical formulation matrix is neat FKM plus 1, 3, and 5 parts graphene nanoplatelets per hundred parts rubber. The exact range should be adjusted after mixing torque and dispersion microscopy. Tensile strength, elongation, tear resistance, hardness, compression set, volume swell, decompression damage, and permeation should be measured before any valve assembly test. Where explosive or rapid gas decompression is credible, the compound and its manufacturing route should be qualified under the applicable project requirements, including NORSOK M 710 when specified [21].

4.5 Graphene oxide phytic acid film for protected antiwax surfaces

Tan et al. reported a one-step functionalized graphene oxide phytic acid coating with high wax inhibition in their waxy oil transportation experiment [20]. The proposed mechanism relied on a hydrated superhydrophilic and underwater oleophobic interface. That mechanism makes the water fraction a controlling variable. It may be valuable for a produced fluid that contains an aqueous phase, but it may not operate in dry oil and may be vulnerable to abrasive solids.

For this reason, the film is classified as exploratory and restricted to protected portions of the bore or cavity where contact stress is negligible. It is explicitly excluded from the ball seat sealing band, the scraper edge, and any surface that can shed particles directly into the interface. A cold finger or flow loop test should compare coated and uncoated substrates at 2 and 5 percent wax, multiple water fractions, and the stated solids concentration. Adhesion and surface chemistry must be remeasured after the erosion exposure.

5 Proposed Functionally Zoned Valve Design

The first prototype should use the smallest number of simultaneous material changes that can still test the zoning concept. The recommended lead configuration is a polished micro nano WC–10Co–4Cr coating on the ball sealing bands and metallic scraper surfaces, a low-loading graphene nanoplatelet PEEK primary seat selected from coupon and creep tests, and an FKM secondary seal selected from neat and graphene-modified compounds. The GO phytic acid film should be omitted from the first pressure qualification valve unless it has already passed a separate adhesion and particle erosion gate. This sequencing isolates causes when leakage or torque changes.

The hard coating should terminate outside the sharpest geometric transition and include a controlled edge radius. Coating allowance must be included in the ball diameter, seat interference, and final lapping plan. The seat support ring should be locally stiffened or radiused if FEA identifies the same stress concentration reported in large valve research [3]. Spring preload should be adjustable in the research prototype so that material effects can be separated from contact pressure. The scraper should remove deposits without forcing debris beneath the primary seat; a relief path or capture cavity should be included downstream of the scraper edge.

Material zoning is linked to the flow field. CFD hot spots on the downstream seat edge should be compared with the physical coating boundary. If a predicted cavitation or particle impact zone crosses from the coated ball to an unprotected substrate, the termination should move, or the geometry should be altered. Likewise, a low-velocity recirculation region that retains wax may justify a drainage or flushing feature before an antiwax surface treatment is considered. The material is therefore the last element of a chain that begins with port geometry and cavity management.

6 Integrated CFD FEA and Materials Selection Framework

6.1 Hydraulic model

The CFD programme should include fully open flow and a set of closing angles that resolve the rapid area contraction region. A practical sequence is 0, 15, 30, 45, 60, 75 and 82 degrees from fully open, with additional angles around the onset of the highest pressure gradient. Steady simulations can screen geometry, but transient closure is required to evaluate pressure waves and time-dependent vapour volume. The model should report pressure loss, minimum static pressure, cavitation volume fraction, wall shear stress, recirculation residence time, and particle impact statistics. Mesh independence must be demonstrated for both global pressure loss and local seat edge velocity.

The field envelope should be run at 50 and 60 °C with fluid property sensitivity. The earlier viscosity entries cannot be used until their units and reference temperatures are confirmed. A credible range should therefore be defined from laboratory rheometry of the oil water wax mixture. Particle size distribution, density, and angularity should also be measured rather than represented only by the concentration of 132 mg per litre. For cavitation, vapour pressure and dissolved gas assumptions should be documented.

6.2 Structural contact model

The nonlinear FEA model should include the ball, both seat rings, primary PEEK components, support rings, springs or preload elements, body stiffness and frictional contacts. Load steps should reproduce assembly preload, pressure from the left, depressurization, pressure from the right, and thermal stabilization. Outputs include minimum and maximum sealing band pressure, its circumferential coefficient of variation, seat deformation, support ring stress, ball displacement, and predicted actuation torque. Temperature-dependent elastic and viscoelastic properties are required for PEEK, while hyperelastic and time-dependent data are required for FKM if the O-ring is represented directly.

A wear update can be implemented after the contact model is validated. Archard-type wear may be used as a comparative numerical law, but its coefficient must be fitted to the same material pair, lubricant, and solids condition as the valve. Geometry should be updated in increments and the contact analysis repeated. The most useful output is the change in continuous sealing width and minimum pressure, not a visually impressive wear contour.

6.3 Evidence gates

Figure 2 organizes the evidence sequence. Each gate can reject a candidate before the next more expensive test. Coupon results provide constitutive data and failure modes; subcomponent tests reproduce curved contacts and edges; prototype testing measures bidirectional leakage and torque; qualification verifies compliance with the applicable valve standard. A material that fails adhesion or creep should not be rescued by proceeding directly to a full valve test.

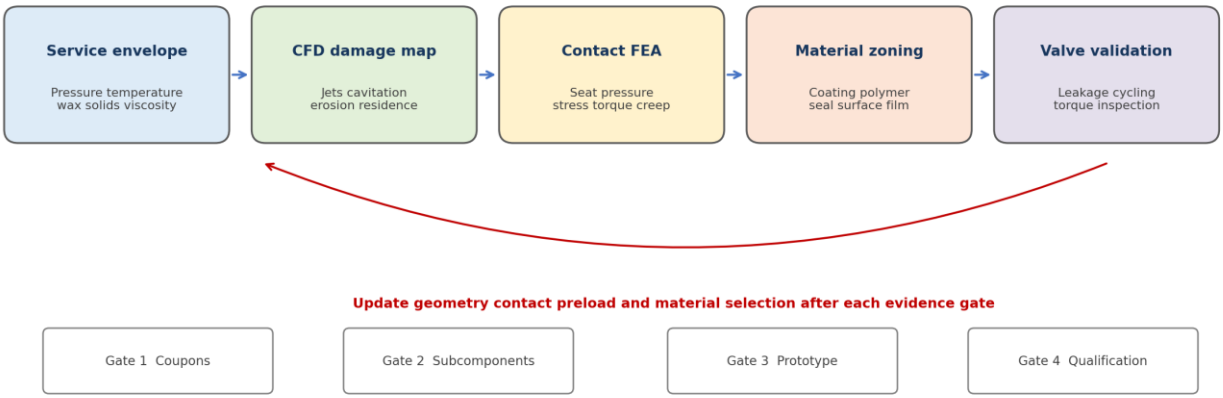


Figure 2 Integrated simulation material selection and evidence gate workflow.

7 Experimental Validation Programme

7.1 Specimen matrix and characterization

Table 3 gives a minimum screening matrix. Replicate count should be set through a power analysis after pilot scatter is known. All coated specimens should be manufactured in more than one spray batch so that the experiment does not confuse a material effect with one batch. Polymer plaques and machined seat segments should be conditioned under the same thermal history as the valve components.

Table 3 Proposed screening matrix with baselines and decision outputs

Component family	Candidate levels	Mandatory baseline	Primary outputs
Ball and scraper coating	Conventional WC–10Co–4Cr micro-nano HVOF fine feedstock HVAF	Qualified production coating or uncoated hardened substrate	Porosity, phases, hardness, toughness, adhesion, residual stress, roughness, cavitation, and slurry loss
Thin film comparator	Nitrided plus DLC CrN CrCN	Nitrided substrate without film	Scratch adhesion, pinholes, friction, edge delamination, cavitation damage
Primary seat	PEEK with 0, 0.5, 1.0, 2.0 mass percent GNP	Production grade neat PEEK	Dispersion modulus, creep recovery, thermal expansion, friction wear, leakage
Primary seat comparator	Neat PEEK and selected hBN or WS_2 PEEK levels	Same neat PEEK batch	Friction wear thermal conductivity machining integrity sealing recovery
Secondary seal	FKM with 0, 1, 3, 5 phr GNP	Qualified production FKM	Dispersion, cure, tensile tear, swelling, compression set, permeation, decompression damage
Antiwax surface	Bare alloy GO phytic acid film	Production bore finish	Contact angle, adhesion, deposit mass and thickness, particle erosion retention

Metallic coatings should be characterized by cross-sectional SEM and EDS, X-ray diffraction, image-based porosity, microhardness or nanoindentation, surface profilometry, and an adhesion method appropriate to coating thickness. Fracture toughness or an indentation crack resistance proxy should supplement hardness. The finished spherical surface must be measured for roughness, waviness, and roundness because a low coupon roughness does not guarantee a continuous sealing band on a large ball.

Polymer and elastomer nanocomposites require dispersion mapping. Optical or electron microscopy, Raman mapping where appropriate, density and thermal analysis should be related to mechanical performance.

PEEK tests should include compressive creep and recovery at 50 and 60 °C under FEA-derived pressure levels. FKM tests should include oil and brine aging, compression set, volume and mass change, hardness change, and microscopy after decompression.

7.2 Tribology cavitation and wax tests

The metallic coating tribometer should reproduce the coated ball against a seat or scraper counterface with representative contact pressure and small-amplitude sliding. Tests are required in base oil, oil with the representative aqueous phase, and oil with 132 mg per litre solids. Friction, wear volume, coating penetration, counterface wear, and debris morphology should be recorded. A test that reports only the wear of the coating can select a coating that destroys the softer seat.

Cavitation screening should begin with ASTM G32 vibratory testing and may be complemented by ASTM G134 cavitating jet testing [22], [23]. These standardized tests rank material resistance under controlled conditions; a valve flow loop is then required to reproduce the hydrodynamic jet, pressure recovery, and particle interaction. Mass loss, volume loss, incubation time and damage morphology should be compared at fixed intervals. Coating failure at the edge or substrate interface is a rejection event even when average mass loss is low.

Wax testing should use a cold finger or temperature-controlled flow loop with the actual or compositionally matched oil. At minimum, 2 and 5 percent wax levels should be crossed with water fraction and surface condition. Deposit mass, thickness, removal force, and residual film chemistry should be recorded. Surface roughness must be controlled because it independently changes wax deposition [7]. The coated specimen should then receive a solids erosion exposure, and the wax test should be repeated to determine whether the antiwax function survives.

7.3 Seat segment and full valve testing

A curved seat segment rig should bridge flat coupons and the DN500 valve. It should reproduce the ball radius, coating finish, seat edge, spring load, temperature, and contaminant exposure. The rig can measure breakaway friction, running friction, leak rate across a short sealing arc, and wear scar evolution. High-speed imaging or acoustic emission may help identify debris generation or coating cracking, but inspection after fixed cycle blocks remains essential.

The full valve sequence should include shell and seat tests, low- and high-pressure bidirectional leakage, torque measurement, thermal stabilization, repeated opening and closing, and periodic leakage checks. The direction of pressure should alternate in a defined sequence so that one seat is not always the upstream seat. After testing, the valve should be disassembled for surface profilometry, microscopy, and dimensional inspection. Fugitive emission performance of the stem sealing system should be tested to ISO 15848- 1 if it is within project scope [24]. Final acceptance remains subject to API 6D and ISO 14313 requirements and to the purchaser specification [1], [2].

Table 4 Decision metrics for progressing from screening to valve qualification

Gate	Progression criterion	Action if not met
Coating integrity	No through-coating cracks, edge chipping, or interface delamination after the specified test block	Reject candidate or modify substrate preparation thickness and edge geometry
Coating surface	Porosity and roughness match or improve the qualified baseline after finishing; spherical form remains within seal tolerance	Reprocess and repeat leakage-relevant surface characterization
Seat contact	Continuous sealing band in both pressure directions; Equation 4 satisfied; contact variation reduced relative to baseline	Adjust support stiffness, spring preload, seat profile or polymer grade
Polymer durability	Creep recovery and wear preserve sealing geometry after thermal and fluid aging	Reject filler level or redesign load path
Elastomer durability	Swelling, compression set elongation, and decompression damage remain within project compound limits	Return to neat FKM or change compound and cure system
Wax control	Deposit and removal force improve against a roughness-matched control after erosion exposure	Keep as exploratory and exclude from prototype

Gate	Progression criterion	Action if not met
Valve function	Bidirectional leakage complies with the specified standard; no progressive torque instability or damaging debris	Identify hydraulic contact or material cause before further cycling

8 Expected Scientific Contribution and Limitations

The proposed scientific contribution is the coupling of a hydraulic damage map with a bidirectional contact pressure map and a functionally zoned nanomaterial selection. Existing studies usually evaluate one coating, one polymer composite, or one valve geometry. The present framework makes the location of a material part of the hypothesis. It predicts that a thick dense carbide coating is more suitable for exposed metallic sealing and scraping zones, a low concentration nanocomposite is more suitable for a compliant primary seat, and a hydrated antiwax film is only credible on a protected noncontact zone. The framework can be falsified if the mapped damage does not coincide with observed failure, if the selected material worsens the counterface, or if valve leakage does not track contact pressure retention.

Several limitations are explicit. First, the literature data were generated on different substrates, fluids, loads, and specimen geometries; their numerical improvements cannot be converted directly into valve life. Second, the field viscosity data require unit confirmation, and the produced fluid particle distribution and water fraction are not yet defined. Third, nanoparticle health and handling controls must be included during compounding, spraying, machining, and waste collection. Fourth, large ball coating scale-up may introduce thickness gradients and residual stresses absent from coupons. Fifth, qualification of a modified seat compound or coating can require manufacturing process control beyond the laboratory formulation.

The design also involves trade-offs. A harder ball coating may increase PEEK wear; a stiffer graphene PEEK seat may reduce extrusion but increase leakage sensitivity to shape error; a lower friction surface may change the self-energizing behaviour of the seat; and a hydrophilic antiwax coating may increase corrosion risk at a defect. These interactions justify the evidence gate sequence and the retention of a conventional qualified baseline in every test campaign.

9 Conclusions

- The valve should be treated as a set of damage zones rather than as one material selection problem. Geometry and contact pressure remain the first design controls, while nanomaterials are used to protect the residual critical zones.
- A polished micro nano WC–10Co–4Cr coating applied by an optimized HVOF or fine feedstock HVAF route is the lead candidate for the ball sealing band and metallic scraper. Nitriding plus DLC and CrN or CrCN should be tested as alternative thin film systems, not automatically stacked over the carbide coating.
- Graphene nanoplatelet PEEK is the lead primary seat screening family, with hBN PEEK or WS_2 PEEK as controlled comparators. Selection must be based on creep recovery and valve leakage as well as friction and wear.
- Graphene-modified FKM is a credible secondary seal research candidate, but oil aging, compression set, dispersion, and rapid gas decompression performance must be established for the actual compound.
- The GO phytic acid antiwax film is exploratory and should be restricted to protected noncontact surfaces until its water fraction dependence, adhesion, and particle erosion durability are proven.
- The 89 mm field screening line and the DN500 PN100 structural valve are separate validation envelopes. The integrated CFD FEA coupon subcomponent and valve programme provides a defensible route from literature evidence to qualified construction without claiming unmeasured performance.

Declarations

Data availability: No new experimental dataset is reported in this design framework. The operating envelopes are project inputs and the cited numerical results remain attributable to the original publications.
Conflict of interest: The author declares no conflict of interest related to this manuscript.

References

[1] International Organization for Standardization. Oil and gas industries including lower carbon energy – Pipeline transportation systems – Pipeline valves. ISO 14313:2025. Geneva: ISO; 2025.
[2] American Petroleum Institute. Specification for valves. 25th ed. API Specification 6D. Washington (DC): American Petroleum Institute; 2021.
[3] LI Q, LI L, CHENG L, YU C, HAN C. Research on two-way sealing performance of fully welded large-caliber ball valve. Journal of Xihua University (Natural Science Edition). 2022 Nov 1;41(6):61-7.
[4] Ivancu LI, Popescu D. Investigation of the fluid flow in a large ball valve designed for natural gas pipelines. Applied Sciences. 2023 Mar 27;13(7):4247. https://doi.org/10.3390/app13074247
[5] Kang HL, Park HJ, Han SH. Investigation of the flow characteristics for cylinder-in-ball valve due to a change in the opening rate. Applied Sciences. 2022 Sep 6;12(18):8930. https://doi.org/10.3390/app12188930
[6] Zhang L, Deng Y, Liu Y, Liu X, Jiang X, Wu D, Wang Z. Failure analysis and wear-life prediction of a deep sea high-pressure ball valve under repeated opening-closing cycles. Engineering Failure Analysis. 2026 Jun 11:111114. https://doi.org/10.1016/j.engfailanal.2026.111114
[7] Burmaster D, Kainer A, Lu Y. Effects of surface roughness on wax deposition. Geoenergy Science and Engineering. 2023 Dec 1;231:212383. https://doi.org/10.1016/j.geoen.2023.212383
[8] Burmaster D, Chaudhry I, Lu Y. Experimental investigation of wax deposition on multiple steel alloys. Geoenergy Science and Engineering. 2024 Aug 1;239:212966. https://doi.org/10.1016/j.geoen.2024.212966
[9] Bobzin K, Heinemann H, Burbaum E, Schulz M. Development of near net shaped coatings for reduced postprocessing costs in valves. Journal of Thermal Spray Technology. 2023 Mar;32(2):681-92. https://doi.org/10.1007/s11666-023-01539-9
[10] Ding X, Cheng XD, Yuan CQ, Shi J, Ding ZX. Structure of micro-nano WC-10Co4Cr coating and cavitation erosion resistance in NaCl solution. Chinese Journal of Mechanical Engineering. 2017 Sep;30(5):1239-47. https://doi.org/10.1007/s10033-017-0162-9
[11] Hong S, Wu Y, Zhang J, Zheng Y, Qin Y, Lin J. Ultrasonic cavitation erosion of high-velocity oxygen-fuel (HVOF) sprayed near-nanostructured WC–10Co–4Cr coating in NaCl solution. Ultrasonics Sonochemistry.2015 Sep 1;26:87-92. https://doi.org/10.1016/j.ultsonch.2015.01.012
[12] Huang Y, Ding X, Yuan CQ, Yu ZK, Ding ZX. Slurry erosion behaviour and mechanism of HVOF sprayed micro-nano structured WC-CoCr coatings in NaCl medium. Tribology International. 2020 Aug 1;148:106315. https://doi.org/10.1016/j.triboint.2020.106315
[13] Cheng F, Jiang S. Cavitation erosion resistance of diamond-like carbon coating on stainless steel. Applied Surface Science. 2014 Feb 15;292:16-26. https://doi.org/10.1016/j.apsusc.2013.11.044
[14] Krella A, Marchewicz A. Effect of mechanical properties of CrN/CrCN coatings and uncoated 1.402 stainless steel on the evolution of degradation and surface roughness in cavitation erosion. Tribology International. 2023 Jan 1;177:107991. https://doi.org/10.1016/j.triboint.2022.107991
[15] Puértolas JA, Castro M, Morris JA, Ríos R, Ansón-Casaos A. Tribological and mechanical properties of graphene nanoplatelet/PEEK composites. Carbon. 2019 Jan 1;141:107-22. https://doi.org/10.1016/j.carbon.2018.09.036
[16] Kalin M, Zalaznik M, Novak S. Wear and friction behaviour of poly-ether-ether-ketone (PEEK) filled with graphene, WS2 and CNT nanoparticles. Wear. 2015 May 1;332:855-62. https://doi.org/10.1016/j.wear.2014.12.036
[17] Yang F, Li J, Han S, Ma N, Li Q, Liu D, Sui G. Wear resistant PEEK composites with great mechanical properties and high thermal conductivity synergized with carbon fibers and h-BN nanosheets. Polymers for Advanced Technologies. 2023 Jul;34(7):2224-34. https://doi.org/10.1002/pat.6043

[18] Liu M, Cataldi P, Young RJ, Papageorgiou DG, Kinloch IA. High-performance fluoroelastomer-graphene nanocomposites for advanced sealing applications. Composites Science and Technology. 2021 Jan 20;202:108592. https://doi.org/10.1016/j.compscitech.2020.108592
[19] Wei J, Jacob S, Qiu J. Graphene oxide-integrated high-temperature durable fluoroelastomer for petroleum oil sealing. Composites science and technology. 2014 Feb 24;92:126-33. https://doi.org/10.1016/j.compscitech.2013.12.010
[20] Tan SL, Von Lau E, Majumder M, Luo R, Wu G. Facile one-step functionalised graphene oxide-phytic acid coating towards effective wax inhibition in waxy oil transportation. Fuel. 2024 Dec 1;377:132829. https://doi.org/10.1016/j.fuel.2024.132829
[21] Standards Norway. NORSOK M-710:2014/AC:2019. Qualification of non-metallic materials and manufacturers – Polymers. Lysaker: Standards Norway; 2019.
[22] ASTM International. Standard test method for cavitation erosion using vibratory apparatus. ASTM G32-16(2021)e1. West Conshohocken (PA): ASTM International; 2021.
[23] ASTM International. Standard test method for erosion of solid materials by cavitating liquid jet. ASTM G134-17. West Conshohocken (PA): ASTM International; 2017.
[24] International Organization for Standardization. Industrial valves – Measurement, test and qualification procedures for fugitive emissions – Part 1: Classification system and qualification procedures for type testing of valves. ISO 15848-1:2015. Geneva: ISO; 2015.